Journal of King Saud University – Science 34 (2022) 102113

Contents lists available at ScienceDirect

Journal of King Saud University – Science

journal homepage: www.sciencedirect.com

Original article

β-sitosterol conjugated silver nanoparticle-mediated amelioration of CCl_4-induced liver injury in Swiss albino mice

Pallab Kar [a], Swarnendra Banerjee [a], Md. Moshfekus Saleh-E-In [b], Akash Anandraj [c], Emil Kormuth [d], Suntheren Pillay [e], Abdullah Ahmed Al-Ghamdi [f], Mohammad Ajmal Ali [f], Joongku Lee [g], Arnab Sen [a,*], Devashan Naidoo [c,*], Ayan Roy [h,*,1], Yong Eui Choi [b,*]

[a] Molecular Cytogenetics Laboratory, Department of Botany, University of North Bengal, Siliguri 734001, India
[b] Division of Forest Resources, College of Forest and Environmental Sciences, Kangwon National University, Chunchon 200701, Republic of Korea
[c] Centre for Algal Biotechnology, Faculty of Natural Sciences, Mangosuthu University of Technology, P.O. Box 12363, Durban 4026, South Africa
[d] Faculty of Natural Sciences, Mangosuthu University of Technology, P.O. Box 12363, Durban 4026, South Africa
[e] Ubuntu People's Powered Solutions, 82 Mazisi Kunene Road, Glenwood, Durban 4001, South Africa
[f] Department of Botany and Microbiology, College of Science, King Saud University, Riyadh 11451, Saudi Arabia
[g] Department of Environment and Forest Resources, Chungnam National University, Daehak-ro, Yuseong-gu, Daejeon, Republic of Korea
[h] Department of Biotechnology, Lovely Professional University, Punjab 144001, India

ARTICLE INFO

Article history:
Received 20 February 2022
Revised 4 May 2022
Accepted 16 May 2022
Available online 20 May 2022

Keywords:
BSAgNPs
Hepatotoxicity
Oxidative stress
Liver fibrosis
Nrf2
TGF-β

ABSTRACT

Objective: Drug induced hepatocyte death is a major contributor to acute liver failure. We aimed to determine whether β-sitosterol conjugated silver nanoparticles (BSAgNPs) could ameliorate carbon tetrachloride (CCl_4)-induced liver injury in Swiss albino mice.
Methods: Biogenic silver nanoparticles were synthesized from β-sitosterol to produce β-sitosterol (BS) conjugated silver nanoparticles. Serum liver function assays in mice model with CCl_4-induced liver injury revealed that alanine aminotransferase (ALT), aspartate aminotransferase (AST), alkaline phosphatase (ALP), bilirubin and cholesterol levels decreased markedly after treatment with β-sitosterol and BSAgNPs. *In vivo* liver enzymatic assays, including superoxide dismutase (SOD), catalase and reduced glutathione (GSH) were conducted to assess the antioxidant activity of the treatments.
Results: Liver tissue from BSAgNP treated mice displayed significantly elevated SOD activity (73.57 ± 1.48%) when compared to positive control group with silymarin treatment. Catalase activity decreased drastically in CCl_4 treated mice (47.14 ± 1.08%), but increased with the administration of BSAgNPs (72.24 ± 2.25%). An increase in transforming growth factor β (TGF-β1) in liver tissue homogenate accompanied a reduction in nuclear factor erythroid-2-related factor 2 (Nrf2) in CCl_4 treated mice. β-sitosterol and BSAgNPs mediated the reduction of TGF-β1. In the BSAgNPs treated mice, Nrf2 level was significantly elevated; however, no change was detected following β-sitosterol treatment.
Conclusion: Our findings reveal that β-sitosterol conjugated silver nanoparticles (BSAgNPs) may cause activation of the Nrf2 gene, through potential inhibition of TGF β1/Smad signaling. Antifibrotic effect of BSAgNPs may promote the lowering of chronic inflammation, oxidative stress and collagen deposition. Nanoparticle-mediated drug delivery of β-sitosterol may therefore have therapeutic promise against hepatic complications.

* Corresponding authors.
E-mail addresses: senarnab_nbu@hotmail.com (A. Sen), naidoo.devashan@mut.ac.za (D. Naidoo), ayanroy.bio@gmail.com (A. Roy), yechoi@kangwon.ac.kr (Y.E. Choi).
[1] Present address: Mailman School of Public Health, Columbia University, New York 10032, USA.

Peer review under responsibility of King Saud University.

Production and hosting by Elsevier

1. Introduction

Drug induced liver injury or hepatotoxicity is an adverse response following the intake of natural products or synthetic drug compounds (Francis and Navarro, 2021). The biochemical mechanism for the development of liver injury is described as being either intrinsic or idiosyncratic (Francis and Navarro, 2021). The drugs implicated in intrinsic liver injury cause hepatocyte death in a dose dependent manner (Francis and Navarro, 2021; Yuan

https://doi.org/10.1016/j.jksus.2022.102113
1018-3647/

and Kaplowitz, 2013). Idiosyncratic liver injury on the other hand is not dose dependent and is rather influenced by host factors (patient age, gender and innate or adaptive immune responses involving the ligands of the tumor necrosis factor family), drug weight, lipophilicity and environmental factors (Francis and Navarro, 2021). Similarities in the clinical presentation of drug-induced liver injury and other hepatobiliary disorders complicate the estimation of the true incidence of hepatotoxicity. However, the most recent reports suggest an annual occurrence of 15–20 cases per 1,00,000 worldwide (Chalasani et al., 2015; Tujios and Lee, 2018). Around 2000 cases of acute liver failure are reported in the US every year and 50% of these cases are associated with drug-induced hepatotoxicity (DIHT) making it the leading cause of acute liver failure (Flora et al., 2008; Fisher et al., 2015). Furthermore, approximately 75% of idiosyncratic drug reactions lead to liver failure resulting in death (Flora et al., 2008). Liver injury has emerged as a global concern and warrants the attention of clinical research and medical interventions.

Halogenated alkenes are organic xenobiotics (carbon tetrachloride; CCl_4) that may cause liver injury and are used to study xenobiotic metabolism (Subramonium and Pushpangadan, 1999; Weber et al., 2003). CCl_4 mediated liver damage is triggered by free radicals that injure parenchyma tissue and cause inflammatory dysregulations. A number of reactive oxygen (ROS) or nitrogen species (RNS) initiate a cascade of intracellular events that induce the release of pro-inflammatory cytokines and promote inflammation signaling (Anderson et al., 1994; Flohe et al., 1997). The radicals formed by the metabolism of CCl_4 cause lipid peroxidation and are implicated in membrane damage (Anderson et al., 1994; Flohe et al., 1997). Repeated cycles of injury and inflammation lead to fibrosis, liver injury and may eventually progress to hepatocellular carcinoma (HCC) (Anderson et al., 1994; Flohe et al., 1997).

β-sitosterol is a phytosterol found in vegetable oils, nuts and avocados and displays antioxidant, anticancer and anti-inflammatory properties (Kim et al., 2012). It has been reported to reduce liver injury, benign prostatic hyperplasia (BPH) and maintain normal blood cholesterol levels (Kim et al., 2012; Rudkowska et al., 2008; Wilt et al., 2000). However, the clinical application of β-sitosterol is challenged by its large molecular weight and low bioavailability. Nanoparticles are highly soluble and chemically inert with low molecular weights. These features establish nanoparticle-based drug delivery approach as a promising solution to this bottleneck in pharmaceutical research (Banerjee et al., 2021). There has been limited knowledge about the applications of β-sitosterol conjugated silver nanoparticles (BSAgNPs) in treating liver injury. Here, we studied the effect of BSAgNPs on CCl_4-induced liver injury in mice. Our study provides substantial evidence for the ameliorative effect of BSAgNPs against liver injury and generates scopes to explore their therapeutic potentials.

2. Materials and methods

2.1. Synthesis

BSAgNPs were synthesized by mixing β-sitosterol (30 mg dissolved in 10 ml of distilled water) and $AgNO_3$ [SN; 1.575 g (0.103 M) dissolved in 90 ml of distilled water]. The solution was boiled at (80 °C) on a magnetic stirrer for 6–8 h eliciting a color change from colorless to greyish-brown. The solution was then centrifuged at 6000 rpm for 20 mins at room temperature. After air-drying the samples were preserved at 4 °C (Banerjee et al., 2021; Kar et al., 2021).

2.2. Characterization

2.2.1. Scanning electron microscope (SEM) and field emission scanning electron microscope (FESEM) analysis

Characterization of surface morphology of β-sitosterol (BS) conjugated silver nanoparticles (BSAgNPs) was achieved using a JEOL SEM (JEOLJSM-IT100InTouchScopeTM, Tokyo, Japan). Mounting and coating (3 nm gold coating) of powdered samples was conducted by using copper mesh and gold sputtering unit, respectively. Detailed morphology of BSAgNPs at the surface under higher magnifications was conducted by FESEM using Carl Zeiss microscope (Carl Zeiss, Germany make; model: SIGMA-0261) with operational settings at 75,000× magnification (Kar et al., 2021).

2.2.2. Energy dispersive X ray spectroscopy (EDX) analysis

EDX for elemental analysis of BSAgNPs was conducted using JEOL SEM equipped with Oxford-EDX software. Samples were mounted on copper mesh and were gold-coated with a gold sputtering unit (Kar et al., 2021).

2.2.3. High-resolution transmission electron microscopy (HRTEM) analysis

HRTEM analysis was conducted to an optimized reaction (at an accelerating voltage 300 kV) to study the morphology of BSAgNPs (Akwu et al., 2021).

2.3. In vivo study

2.3.1. Toxicity study

Acute toxicity of the β-sitosterol and β-sitosterol conjugated silver nanoparticles (BSAgNPs) was investigated based on OECD guidelines. Briefly, 12 mice (2 mice/group/dose) were made to ingest solutions of β-sitosterol and BSAgNPs at increasing concentrations (500, 1000 and 2000 mg/kg body weight). All mice were stringently monitored to identify the onset of toxicological symptoms (30 mins and then 2, 4, 8, 24, 48, 72 and 96 h).

2.3.2. Animals and care

All *in vivo* experiments were conducted on six or seven-week-old male Swiss albino mice (22 ± 2 gm body weight). The mice (n = 6) were maintained in polypropylene side cage bins, that were housed in individual ventilated cages under control condition (25 °C, 12 h dark/light photoperiod) with access to food and water ad libitum. The experiments, approved by the ethical committee, were conducted as per the animal maintenance rules.

2.3.3. Drug treatment

Thirty male Swiss albino mice were separated into 5 groups of 6 that were exposed to the following treatments;

Group I: control animals (healthy mice); received normal saline water; Group II: Negative control animals; 1:1 (v/v) CCl_4 in olive oil; Group III: Positive control animals; 1:1(v/v) CCl_4 in olive oil as well as 100 mg/kg body weight silymarin; Group IV: 1:1 (v/v) CCl_4 in olive oil as well as β-sitosterol (200 mg/kg/day body weight); Group V: 1:1 (v/v) CCl_4 in olive oil as well as BSAgNPs (200 mg/kg/day body weight). All the treatments were administered orally for 21 days.

Mice were anesthetized with ether (2%) 24 h after the last dose and their hearts were punctured. Blood was collected in a tube containing EDTA, following which all mice were sacrificed. Blood was incubated at room temperature (25 °C) for 60 mins to allow clotting after which we collected serum by centrifugation at 1000 rpm for 60 mins, and then conducted the biochemical analysis. Subsequently, the liver from mice were removed and washed

with phosphate buffer saline. Histological studies were performed on the liver tissue after preservation in 10% formaldehyde solution.

2.3.4. Serum biomarkers for liver function tests

The levels of total bilirubin, cholesterol, albumin, alanine aminotransferase (ALT), aspartate aminotransferase (AST) and alkaline phosphatase (ALP) in the serum samples were estimated using commercially available kits (Crest Biosystems, India).

2.3.5. SOD, Catalase, GSH and lipid peroxidation activity

The activities of SOD, CAT and GSH activity were measured following our previous protocol (Kar et al., 2019). Malondialdehyde was quantified using TBARS assay kit (Cayman, USA).

2.4. ELISA measurements

TGF-β1 and NRF2 in the liver tissue homogenate were measured using ELISA kit (Ray Bio, USA).

2.5. Histopathological examination

For microscopic analysis, liver tissue from treated mice was fixed in formaldehyde (10%) for a period of 24 h and dehydrated. Samples were subsequently embedded in paraffin and a microtome was used to cut the samples into sections (4 μm). The staining procedure comprised of an initial basic staining with hematoxylin for 40 sec followed by an acidic staining (eosin) for 20 sec. Sections were placed on slides and were observed (100X) using an Olympus (model no.: CX21iLEDFS1) microscope.

2.6. Statistical analyses

The KyPlot software (version 5.0) was used to perform statistical test. Dunnett's test was employed to perform the one-way analysis of variance (ANOVA) significance level at $P < 0.05$.

3. Results and discussion

3.1. Characterization

3.1.1. Scanning electron microscope (SEM) and field emission scanning electron microscope (FESEM) analysis

The morphology of β-sitosterol (BS) conjugated silver nanoparticles (BSAgNPs) at the surface was examined using SEM and FESEM. SEM images (Fig. 1) indicated that synthesized silver nanoparticles were predominantly spherical and oblong. FESEM images (Fig. 2) also supported the images of SEM and an in-depth analysis indicated that particle size varied between 15 and 50 nm. Our SEM and FESEM analysis revealed that the nanoparticles were almost evenly distributed (Banerjee et al., 2021).

3.1.2. Energy dispersive X ray spectroscopy (EDX) analysis

EDX analysis was performed to identify the elements in BSAgNPs (Fig. 3). Despite various peaks, this spectrum showed a distinct peak at ~ 3Kev, representing Ag. Several other elements such as C, O, Mg, Al and S were also identified. Carbon and oxygen are most likely from organic compounds and these elements have been identified as important bio-reducers of Ag^+ to form elemental Ag (AgNPs) (Kabir et al., 2020).

3.1.3. High-resolution transmission electron microscopy (HRTEM) analysis

The spherical nature of BSAgNPs that ranged in sizes between 10 and 40 nm was depicted by HRTEM and the nanoparticles were dispersed with very few agglomerations (Fig. 4). A previous study

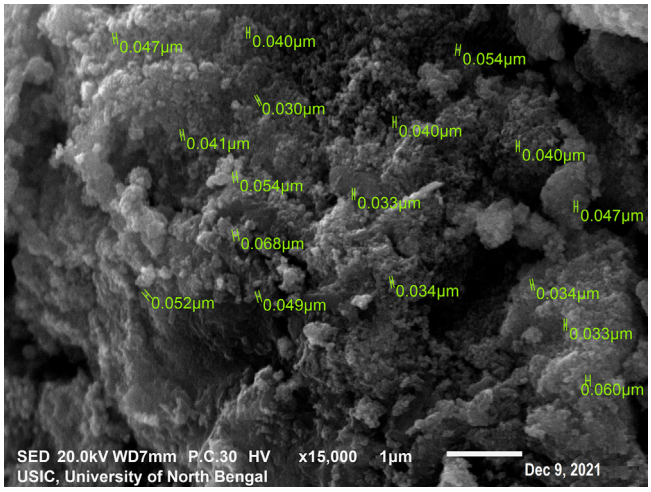

Fig. 1. SEM analysis of BSAgNPs.

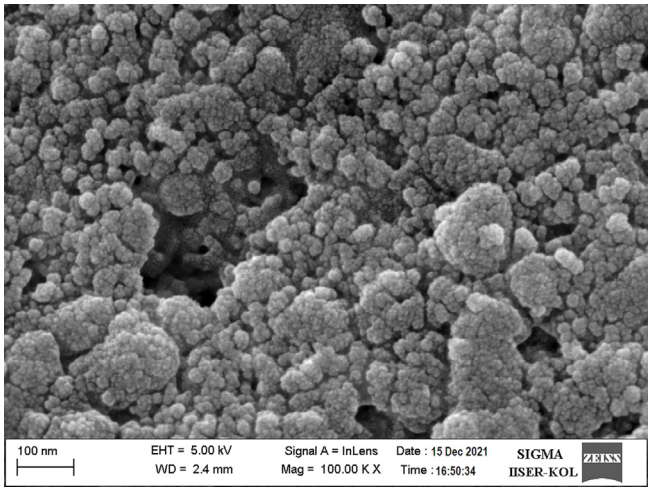

Fig. 2. FESEM analysis of BSAgNPs.

reported that size of a nanoparticle is inversely associated with its bioactivity (Banerjee et al., 2021). As such, our synthesis experiments producing smaller nanoparticles suggest the potential of their improved biological activities.

3.2. In vivo study

3.2.1. Toxicity study

After treatment of β-sitosterol and BSAgNPs on experimental mice, no fatality was observed at 2000 mg/kg dose. So, 1/10th of the ultimate doses were deliberated as safe for *in-vivo* exercise. Oral administration of β-sitosterol and BSAgNPs showed no adverse effect on experimental mice behavior, stool frequency and color. Our observations are consistent with previous studies reporting the non-toxic nature of β-Sitosterol conjugated Poly (lactide-co-glycolic acid) and block copolymers of Poly (ethylene glycol)-block-poly (lactic acid) nanoparticles (Andima et al., 2018; Rajavel et al., 2017).

3.2.2. Body weight

Changes in mice body weight following oral administration of CCl_4, silymarin, β-sitosterol and nanoparticle treatments are shown in Table 1. Mice of the control group gained 10.22% in weight while CCl_4 treated mice (negative control) lost 14.60% in weight due to

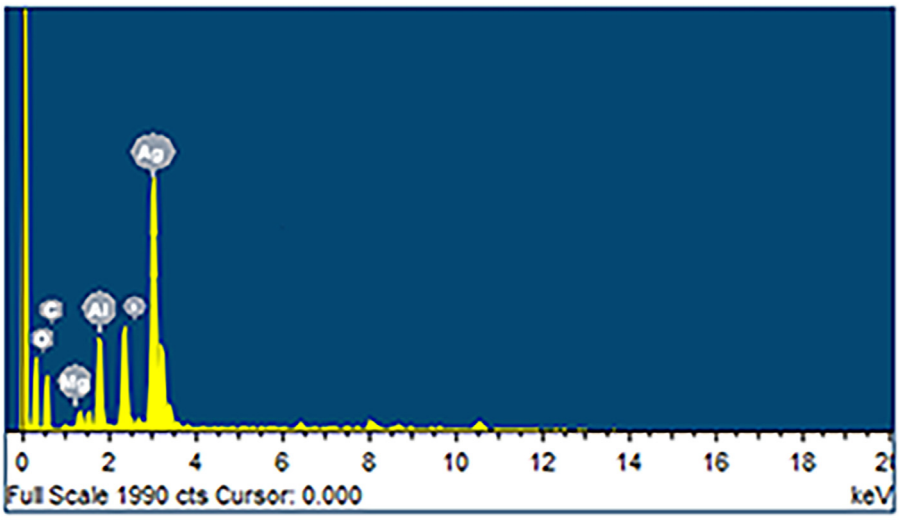

Fig. 3. EDX spectra analysis of BSAgNPs.

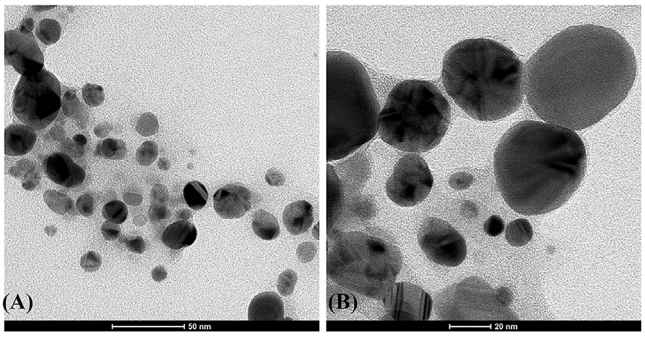

Fig. 4. HRTEM analysis of of BSAgNPs.

liver ailments. The positive control (silymarin) mice group gained 11.02% in weight. Surprisingly, all mice that were treated with β-sitosterol and biogenically synthesized BSAgNPs gained weight. It was interesting to note that mice treated with BSAgNPs gained more weight than those that were treated with β-sitosterol. A significant increase in liver weight was recorded for CCl_4 treated mice potentially due to increase accumulation of fat vacuoles, increased hepatic cholesterol and triglyceride levels (Nan et al., 2000). In a previous study, Nan and colleagues demonstrated a significant increase in relative liver weights in rats with liver fibrosis induced by biliary obstruction as a result of the accumulation of hepatic hydroxyproline after surgery (Nan et al., 2000). CCl_4 toxicity leads to transport of fats from peripheral adipose tissue to the liver, resulting in an increased liver weight and decreased adipose tissue weight (Nan et al., 2000).

3.2.3. Serum liver function markers assay

The results pertaining to the serum liver function assays in the experimental mice are presented in Table 2. The control group exhibited normal ALT, AST, ALP, bilirubin, cholesterol and albumin levels. However, in CCl_4 treated mice, ALT, AST, ALP, bilirubin and cholesterol levels increased while the level of albumin decreased when compared to control animals. It was interesting to note that ALT, AST, ALP, bilirubin and cholesterol levels were markedly decreased following treatment with β-sitosterol and BSAgNPs, a pattern consistent with the positive control group treated with silymarin. In a previous study curcumin treatment led to decreased levels of liver injury in mice model, and has been suggested to inhibit lipid peroxidation and protect membrane damage (Naik et al., 2011). Our data suggest that treatment with BSAgNPs might be protective against hepatic damage induced by CCl_4 treatment.

3.2.4. In vivo antioxidant assays

The overall antioxidant status was reflected by the elevated SOD, catalase and GSH activities. The β-sitosterol conjugated silver nanoparticles (BSAgNPs) showed elevated SOD activity (73.57 ± 1.48%) significantly when compared to negative control CCl_4 (Fig. 5A) ($p < 0.05$). The catalase activity decreased drastically in CCl_4 treated mice (47.14 ± 1.08%); however, it was noted to increase significantly (72.24 ± 2.25%) (Fig. 5B) ($p < 0.05$) with the administration of BSAgNPs. Similar results were recorded for GSH activity (Fig. 5C) ($p < 0.05$). It was interesting to note that in all the cases β-sitosterol conjugated silver nanoparticles (BSAgNPs) showed better efficacy over the CCl_4 + β-sitosterol group. The MDA level increased significantly with the administration of CCl_4 (79.0 ± 1.41 mM/lit), whereas BSAgNPs lowered the MDA level significantly in CCl_4 treated mice (44.0 ± 5.65 mM/lit) (Fig. 5D) ($p < 0.05$).

Antioxidants have become an important line of defense against CCl_4-induced hepatotoxicity as inhibitors of free radicals and their production (Latha et al., 2009; Feng et al., 2011). SOD, catalase and GSH play diverse and important roles in preventing and neutralizing free radical-induced damage. For instance, SOD lowers the steady-state level of O_2^* while GPx catalyses the production of glu-

Table 1
Body weight (g) and liver weight (g) in the different treatment groups of mice.

Group	Initial Weight	Final Weight	% body weight change	Liver weight	Relative liver weight
Control	22.68 ± 0.12	25.27 ± 0.79	10.22 ± 0.17▲	5.12 ± 0.19	19.83 ± 0.45
CCl_4	22.09 ± 0.09	18.86 ± 0.91	14.60 ± 4.48▼	6.67 ± 0.54	34.08 ± 0.76
Silymarin	22.49 ± 0.09	25.28 ± 0.36	11.02 ± 1.63▲	4.98 ± 0.33	20.19 ± 0.71
CCl_4 + β-sitosterol	23.36 ± 0.37	24.18 ± 0.09	3.37 ± 1.15▲	5.34 ± 0.76	16.04 ± 1.01
CCl_4 + BSAgNPs	22.61 ± 0.08	25.52 ± 0.18	11.38 ± 1.48▲	4.93 ± 0.56	20.05 ± 0.95

BSAgNPs: β-sitosterol silver nanoparticle; Weight (mean ± SD) in gram. ▲ Increase weight; ▼ Decrease weight.

Table 2
Effects of Silymarin, β-sitosterol and BSAgNPs on serum liver function parameters.

Group	Parameters					
	ALT (u/ml)	AST (u/ml)	ALP (u/ml)	Bilirubin (mg/dL)	cholesterol (mg/dL)	albumin (g/dL)
Control	46.51 ± 0.33	59.22 ± 0.11	17.87 ± 0.76	1.03 ± 0.07	72.44 ± 0.49	5.31 ± 0.33
CCl_4	147 ± 0.56	139.67 ± 0.59	39.44 ± 0.71	2.78 ± 0.04	126.03 ± 0.35	2.54 ± 0.06
Silymarin	52.33 ± 0.45	77.76 ± 1.23	20.29 ± 0.23	1.66 ± 0.56	85.22 ± 1.12	4.65 ± 1.10
CCl_4 + β-sitosterol	65.23 ± 1.01	95.11 ± 0.45	31.03 ± 1.10	2.04 ± 0.06	103.21 ± 0.55	3.14 ± 0.05
CCl_4 + BSAgNPs	55.05 ± 0.89	83.78 ± 0.67	26.66 ± 0.35	1.85 ± 0.34	91.52 ± 1.16	4.45 ± 0.87

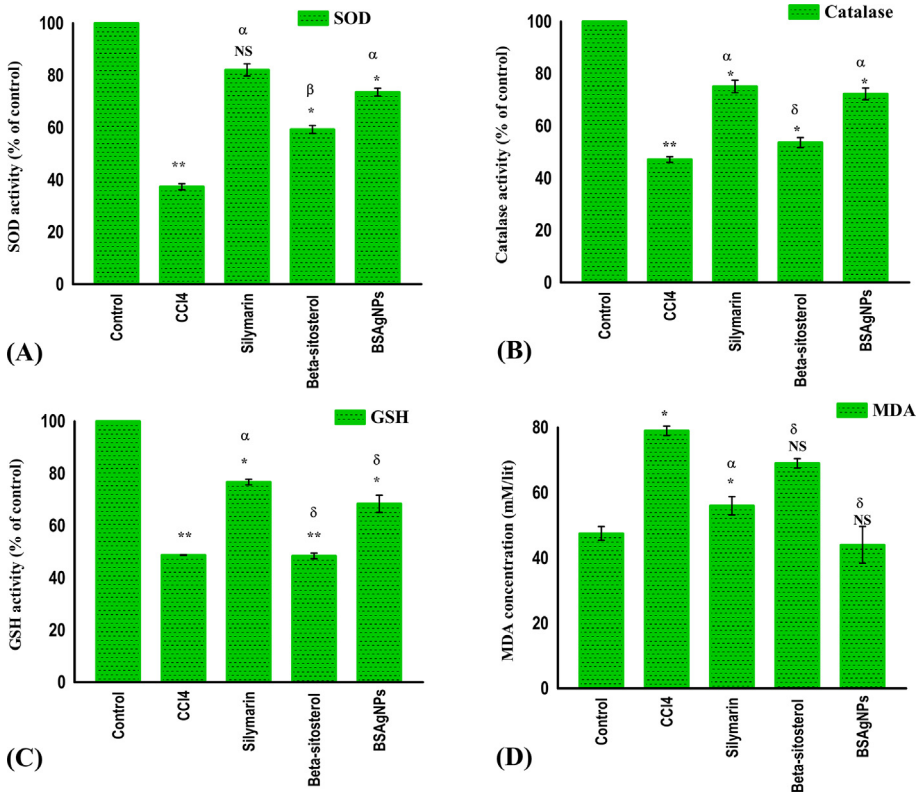

Fig. 5. The effect of β-sitosterol and β-sitosterol conjugated silver nanoparticles (BSAgNPs) on CCl_4 induced liver injury (A) SOD (B) Catalase (C) GSH and (D) MDA activity. [Data expressed as mean ± S.D. (n = 6).*p < 0.05; **p < 0.01; ***p < 0.001; ****p = non significant vs control group; αp < 0.05; βp < 0.01; γp < 0.001; δp = non significant vs CCl_4 group].

tathione disulphide (GSSG) (De Groot and Sies, 1989). Toxic compounds are removed from the liver by conjugation with glutathione, a process mediated by glutathione S-transferases (GST). GR regulates the cellular level of GSH (especially in the reduced state) by eliciting a quick reduction of oxidized glutathione to the reduced form. In CCl_4-induced hepatotoxicity, hepatic necrosis occurs when antioxidant defenses are not produced in sufficient quantities to neutralize ROS production (Masuda and Nakamura, 1990; De Groot and Sies, 1989). Additionally, the metabolism of CCl_4 by hepatic cytochrome P_{450} yields CCl_3, a toxic reactive free radical that causes lipid peroxidation and threatens cellular integrity (De Groot and Sies, 1989; Kiezcka and Kappus, 1980).

3.3. ELISA measurements

The levels of nuclear factor erythroid-2-related factor 2 (Nrf2) and transforming growth factor β (TGF-β) levels in hepatic tissue of mice representing the treatments groups have been depicted in Fig. 6. The levels of TGF-β increased significantly in CCl_4 treated mice compared to control group ($p < 0.05$). However, level of TGF-β decreased in the positive control group treated with silymarin, and the groups representing CCl_4 treated mice administered with β-sitosterol and BSAgNPs. The group treated with BSAgNPs displayed more decreased levels than the one treated with silymarin and β-sitosterol ($p < 0.05$) (Fig. 6B). The group treated with CCl_4 showed significant decrease in levels of Nrf2 in comparison to control group ($p < 0.05$). We did not find any significant change in levels of Nrf2 after silymarin and β-sitosterol treatment; however, administration of BSAgNPs in CCl_4-treated mice group drastically increased Nrf2 levels ($p < 0.05$) (Fig. 6A).

CCl_4-induced oxidative stress promotes liver fibrosis, renal inflammation and collagen synthesis. Reactive oxygen species (ROS) induces lipid peroxidation in liver tissues, damages mitochondrial integrity, and inhibits the electron transport system (ETS) which ultimately culminate in liver fibrosis (Abdullah et al., 2021; Xu et al., 2008). In this experiment, mice treated with BSAgNPs displayed a significant increase in Nrf2 levels. Our data suggest that BSAgNPs may upregulate Nrf2. TGF-β is a prime pacemaker of fibrogenesis (Frangogiannis, 2020; Supriono et al., 2019). Binding of TGF-β with the TGF-βR1 receptor, at the site of injury (hepatic injury), leads to the phosphorylation of Smad2/3 proteins and induces the TGF-β/Smads signaling pathway (Walton et al.,

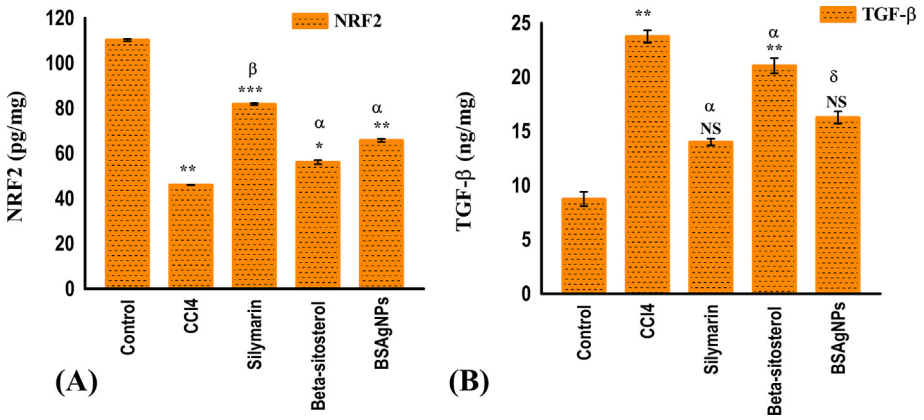

Fig. 6. Effects of silymarin, β-sitosterol and BSAgNPs on the levels of (A) NRF2 and (B) TGF-β1 in hepatic tissue homogenate.

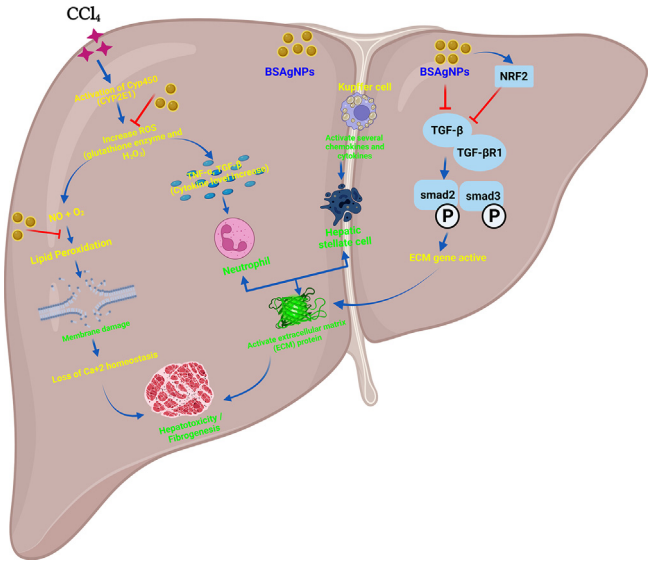

Fig. 7. Detailed mechanism of CCl_4-induced liver injury and its amelioration through BSAgNPs.

2017). These signaling events drive the expression of extracellular matrix (ECM) components that cause deposition of ECM proteins and thickening of tissue, and finally culminate in fibrosis, cell death and organ dysfunction (Walton et al., 2017). Our findings are consistent with the fact that BSAgNPs may suppress the TGF-β signaling (Walton et al., 2017). The Nrf2 gene regulates TGF β1/Smad signaling (Frangogiannis, 2020; Niu et al., 2016). ROS generated by CCl_4 treatment inhibits Nrf2 and leads to the activation of the TGF β1/Smad signaling (Frangogiannis, 2020; Huang et al., 2015). Our data provide evidence that administration of BSAgNPs in the CCl_4 treated mice group increases the levels of Nrf2 with potential inhibition of the TGF β1/Smad signaling and encourage future investigations to have detailed mechanistic insights. The overall mechanism of BSAgNPs-induced amelioration of hepatic injury has been illustrated as Fig. 7.

3.4. Histopathological examination

A histological examination was conducted to examine the degree of damage to liver tissue under the different treatment regimes. Hepatocyte death as a consequence of CCl_4 metabolism results from lipid peroxidation (Basu, 2003). The process triggers

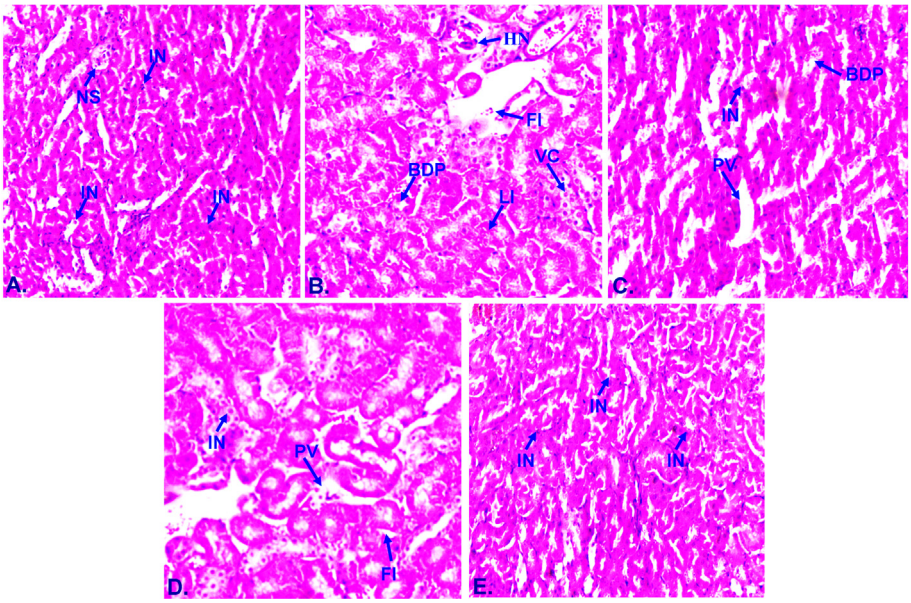

Fig. 8. Histology of control and treated mice liver. (A) Control (B) CCl_4 (C) Silymarin (D) CCl_4 + β-sitosterol (E) CCl_4 + BSAgNPs. [intact nucleus (IN), normal sinusoids (NS), fatty infiltrations (FI), leukocyte infiltrations (LI), congested vesicles (VC), bile duct proliferations (BdP), haemorrhagic necrosis (HN), portal veins (PV)].

inflammation and leads to hepatic fibrogenesis. Microscopic analysis of liver sections taken from control and silymarin treated animals revealed normal structural development of sinusoids (NS) as well as healthy hepatocytes (IN) and a portal vein devoid of inflammation (PV) (Fig. 8A and C). On the other hand, mice treated with $CC1_4$ exhibited several morphological defects including abnormal hepatocellular architecture that upon further examination revealed prominent fatty infiltration sites (FI). These mice also presented bile duct proliferation, vascular congestion and haemorrhagic necrosis (Fig. 8B). These effects are consistent with the toxic effects of CCl_4 metabolism; the metabolites of which lead to ROS generation, and impair mitochondrial integrity and functions leading to the injury of liver cells (Nevin and Vijayammal, 2005). It was interesting to note that mice exposed to BSAgNPs restored the injury more effectively to its normal form (Fig. 8E) when compared to β-sitosterol treated group (Fig. 8D). Our results indicate that administration of BSAgNPs in CCl_4 treated mice might ameliorate the liver injury induced by CCl_4 treatment.

4. Conclusions

In this study, we successfully synthesized and characterized β-sitosterol conjugated silver nanoparticles (BSAgNPs). Our study provides substantial evidence for the antioxidant and hepatoprotective potentials of these nanoparticles in mice model with CCl_4-induced liver injury. Our findings reveal that BSAgNPs administration may inhibit TGF β1/Smad signaling through the upregulation of Nrf2 and confers protection against CCl_4-induced liver injury by restoring the integrity of hepatic cells. Our study generates scopes to explore the therapeutic promise of these nanoparticles in treating liver injury.

Declaration of Competing Interest

The authors declare that they have no known competing financial interests or personal relationships that could have appeared to influence the work reported in this paper.

Acknowledgements

MMSEI and YEC acknowledges Brain Pool Program through the National Research Foundation of Korea (NRF) (Grant number: 2019H1D3A1A01071150). SB is thankful to CSIR, India for fellowship. The authors extend their sincere appreciation to the Researchers Supporting Project number (RSP-2021/306), King Saud University, Riyadh, Saudi Arabia. AS thanks West Bengal Government for Biswa Bangla Genome Centre.

References

Abdullah, A.S., El Sayed, I.E.T., El-Torgoman, A.M.A., Alghamdi, N.A., Ullah, S., Wageh, S., Kamel, M.A., 2021. Preparation and characterization of silymarin-conjugated gold nanoparticles with enhanced anti-fibrotic therapeutic effects against hepatic fibrosis in rats: role of microRNAs as molecular targets. Biomedicines 9, 1767.

Akwu, N.A., Naidoo, Y., Singh, M., Nundkumar, N., Daniels, A., Lin, J., 2021. Two temperatures biogenic synthesis of silver nanoparticles from Grewia lasiocarpa E. Mey. ex Harv. leaf and stem bark extracts: characterization and applications. BioNanoSci. 11, 142–158.

Anderson, M.T., Staal, F.J.T., Gitler, C., Herzenberg, L.A., 1994. Separation of oxidant-initiated and redoxregulated steps in the NF- B signal transduction pathway. Proc. Natl. Acad. Sci. 91, 11527–11531.

Andima, M., Costabile, G., Isert, L., Ndakala, A.J., Derese, S., Merkel, O.M., 2018. Evaluation of β-sitosterol loaded PLGA and PEG-PLA nanoparticles for effective treatment of breast cancer: preparation, physicochemical characterization, and antitumor activity. Pharmaceutics 10, 232.

Banerjee, S., Islam, S., Chattopadhyay, A., Sen, A., Kar, P., 2021. Synthesis of silver nanoparticles using underutilized fruit Baccaurea ramiflora (Latka) juice and its biological and cytotoxic efficacy against MCF-7 and MDA-MB 231 cancer cell lines. S. Afr. J. Bot.

Basu, S., 2003. Carbon tetrachloride-induced lipid peroxidation: eicosanoid formation and their regulation by antioxidant nutrients. Toxicol. 189, 113–127.

Chalasani, N., Bonkovsky, H.L., Fontana, R., Lee, W., Stolz, A., Talwalkar, J., Reddy, K. R., Watkins, P.B., Navarro, V., Barnhart, H., Gu, J., Serrano, J., 2015. United States drug induced liver injury network. Features and outcomes of 899 patients with drug-induced liver injury: the DILIN prospective study. Gastroenterol. 148, 1340–1352.

De Groot, H., Sies, H., 1989. Cytochrome P-450, reductive metabolism, and cell injury. Drug Metab. Rev. 20, 275–284.

Feng, Y., Wang, N., Ye, X., Li, H., Feng, Y., Cheung, F., Nagamatsu, T., 2011. Hepatoprotective effect and its possible mechanism of Coptidis rhizoma aqueous extract on carbon tetrachlorideinduced chronic liver hepatotoxicity in rats. J. Ethnopharmacol. 138, 683–690.

Fisher, K., Vuppalanchi, R., Saxena, R., 2015. Drug-induced liver injury. Arch. Pathol. Lab Med. 139, 876–887.

Flohe, L., Brigelius-Flohe, R., Saliou, C., Traber, M.G., Packer, L., 1997. Redox regulation of NF-κB activation. Free Radic. Biol. Med. 22, 1115–1126.

Flora, S.J., Mittal, M., Mehta, A., 2008. Heavy metal induced oxidative stress and its possible reversal by chelation therapy. Indian J. Med. Res. 128, 501–523.

Francis, P., Navarro, V.J., 2021. Drug Induced Hepatotoxicity. Stat Pearls [Internet]. StatPearls Publishing, Treasure Island (FL).

Frangogiannis, N.G., 2020. Transforming growth factor–β in tissue fibrosis. J. Exp Med, 217.

Huang, W., Li, L., Tian, X., Yan, J., Yang, X., Wang, X., Liao, G., Qiu, G., 2015. Astragalus and Paeoniae radix rubra extract inhibits liver fibrosis by modulating the transforming growth factorβ/Smad pathway in rats. Mol. Med. Rep. 11, 805–814.

Kabir, M.F., Ullah, A.A., Ferdousy, J., Rahman, M.M., 2020. Anticancer efficacy of biogenic silver nanoparticles in vitro. SN Appl. Sci. 2, 1–8.

Kar, P., Banerjee, S., Chhetri, A., Sen, A., 2021. Synthesis, physicochemical characterization and biological activity of synthesized Silver and Rajat Bhasma nanoparticles using Clerodendrum inerme. J. Phytol. 13, 64–071.

Kar, P., Chakraborty, A.K., Dutta, S., Bhattacharya, M., Chaudhuri, T.K., Sen, A., 2019. Fruit juice of silverberry (Elaeagnus) and bayberry (Myrica) may help in combating against kidney dysfunctions. Clin. Phytosci. 5 (1), 1–9.

Kiezcka, H., Kappus, H., 1980. Ox.ygen dependence of CCl4-induced lipid peroxidation in vitro and in vivo. Toxicol. Lett. 5, 191–196.

Kim, T.H., Lim, H.J., Kim, M.S., Lee, M.S., 2012. Dietary supplements for benign prostatic hyperplasia: An overview of systematic reviews. Maturitas 73, 180–185.

Latha, T.B., Srikanth, A., Kumar, E.K., Srinivasa, M.S.K., Rao, Y., Bhavani, B., 2009. Comparative hepatoprotective efficacy of Kumaryasava and livfit against carbon tetrachloride induced hepatic damage in rats. Pharmacol. Online 1, 1127–1134.

Masuda, Y., Nakamura, Y., 1990. Effects of oxygen deficiency and calcium omission on carbon tetrachloride hepatotoxicity in isolated perfused livers from phenobarbital-pretreated rats. Biochem. Pharmacol. 40, 1865–1876.

Naik, S.R., Thakare, V.N., Patil, S.R., 2011. Protective effect of curcumin on experimentally induced inflammation, hepatotoxicity and cardiotoxicity in rats: Evidence of its antioxidant property. Exp. Toxicol. Pathol. 63, 419–431.

Nan, J.X.E.J., Park, H.C., Kang, P.H., Park, J.Y., Kim, D.H., 2000. Antifibrotic effects of a hot-water extract from Salvia miltiorrhiza roots on liver fibrosis induced by biliary obstruction in rats. J. Pharm. Pharmacol. 53, 197–204.

Nevin, K.G., Vijayammal, P.L., 2005. Effect of Aerva lanata against *hepatotoxicity of carbon tetrachloride in rats*. Environ Toxicol Pharmacol. 20, 471–477.

Niu, L., Cui, X., Qi, Y., Xie, D., Wu, Q., Chen, X., Ge, J., Liu, Z., 2016. Involvement of TGF-β1/Smad3 signaling in carbon tetrachloride-induced acute liver injury in mice. PLoS ONE 11, e0156090.

Rajavel, T., Mohankumar, R., Archunan, G., Ruckmani, K., Devi, K.P., 2017. Beta sitosterol and Daucosterol (phytosterols identified in Grewia tiliaefolia) perturbs cell cycle and induces apoptotic cell death in A549 cells. Sci. Rep. 7, 3418.

Rudkowska, I., AbuMweis, S.S., Nicolle, C., Jones, P.J., 2008. Cholesterol-lowering efficacy of plant sterols in low-fat yogurt consumed as a snack or with a meal. J. Am. Coll. Nutr. 27, 588–595.

Subramonium, A., Pushpangadan, P., 1999. Development of phytomedicines for liver diseases. Indian J. Pharmacol. 31, 166–175.

Supriono, S., Nugraheni, A., Kalim, H., Eko, M.H., 2019. The effect of curcumin on regression of liver fibrosis through decreased expression of transforming growth factor-β1 (TGF-β1). Indones. Biomed. J. 11, 52–58.

Tujios, S.R., Lee, W.M., 2018. Acute liver failure induced by idiosyncratic reaction to drugs: Challenges in diagnosis and therapy. Liver Int. 38, 6–14.

Walton, K.L., Johnson, K.E., Harrison, C.A., 2017. Targeting TGF-β mediated SMAD signaling for the prevention of fibrosis. Front. Pharmacol. 8, 461.

Weber, L.W., Boll, M., Stampfl, A., 2003. Hepatotoxicity and mechanism of action of haloalkanes: Carbon tetrachloride as a toxicological model. Crit. Rev. Toxicol. 33, 105–136.

Wilt, T., Ishani, A., MacDonald, R., Stark, G., Mulrow, C., Lau, J., 2000. Beta-sitosterols for benign prostatic hyperplasia. The Cochrane Database Syst. Rev. 2011, CD001043.

Xu, W., Hellerbrand, C., Koehler, U.A., Bugnon, P., Kan, Y.W., Werner, S., Beyer, T.A., 2008. The Nrf2 transcription factor protects from toxin-induced liver injury and fibrosis. Lab. Investig. 88, 1068–1078.

Yuan, L., Kaplowitz, N., 2013. Mechanisms of drug-induced liver injury. Clin. Liver Dis. 17, 507–518.